

# A Non-Invasive Flexible Glucose Monitoring Sensor Using a Broadband Reject Filter

Moussa Bteich , Jessica Hanna , Joseph Costantine , *Senior Member, IEEE*,  
Rouwaida Kanj , *Senior Member, IEEE*, Youssef Tawk , Ali H. Ramadan , and Assaad A. Eid 

**Abstract**—In this paper, a novel, highly accurate, non-invasive glucose-monitoring sensor that is based on a flexible broadband reject filter is presented. The filter topology comprises a tapered feed line at a top layer that excites four open loop resonators on the bottom layer. The broadband reject response is achieved by relying on a modified log-periodic distribution of the open loop resonators. The embedded resonators are reduced in size and are designed to exhibit an enhanced sensitivity to track the variations of the glucose level across the 1.25–2.65 GHz frequency span. The proposed flexible filter is tested within in-vitro, ex-vivo and in-vivo setups. A high correlation between the scattering parameters of the proposed sensor and the variations in glucose levels is attained. Regression models are developed using experimental data obtained from healthy patients that are subjected to glucose tolerance tests. Results demonstrate less than 4% mean absolute relative difference between the reference and estimated glucose levels, and the predicted glucose levels lie 100% within the clinically acceptable zones as shown by the Clarke Error Grid analysis.

**Index Terms**—Broadband reject filter, Clarke error grid, clinical trials, dielectric characterization, non-invasive glucose monitoring sensor.

## I. INTRODUCTION

**D**URING the past few decades, changes in lifestyle and nutrition made diabetes one of the most prominent diseases among chronic conditions. In 2019, the number of patients diagnosed with diabetes exceeded 425 million worldwide, resulting in more than 4 million deaths. This exponentially growing number is expected to reach 629 million by 2045 [1]. In fact, diabetes as a pandemic is one of the most common metabolic diseases. There are two main types of diabetes: type 1 and type 2, with type 1 being the most serious condition [2]. Although the underlying causes of these two categories are different, their consequences are dangerous and much alike [3]. To maintain

Manuscript received February 19, 2020; revised April 18, 2020, July 15, 2020, and August 8, 2020; accepted September 3, 2020. Date of publication September 9, 2020; date of current version May 21, 2021. This work was supported in part by Lebanese National Council for Scientific Research CNRS and in part by UK Lebanon Tech Hub (UKLTH). (*Corresponding author: Joseph Costantine.*)

Moussa Bteich, Joseph Costantine, Rouwaida Kanj, Youssef Tawk, and Ali H. Ramadan are with the Electrical and Computer Engineering Department, American University of Beirut, Beirut 1107 2020, Lebanon (e-mail: msb24@mail.aub.edu; jcostantine@ieee.org; rk105@aub.edu.lb; yatawk@ieee.org; ramadan@ieee.org).

Jessica Hanna is with the Biomedical Engineering Program, American University of Beirut, Beirut 1107 2020, Lebanon (e-mail: jjh21@mail.aub.edu).

Assaad A. Eid is with the Department of Anatomy, Cell Biology and Physiological Sciences, American University of Beirut, Beirut 1107 2020, Lebanon (e-mail: ae49@aub.edu.lb).

Digital Object Identifier 10.1109/JERM.2020.3023053

a proper treatment, accurate determination of blood glucose levels (BGL) is a necessity. Currently, BGL is measured using a glucometer that is invasive and relies on finger pricking several times a day. On the long term, this increases the risk of infection and may damage the underlying tissue. More importantly, this measurement technique does not provide continuous monitoring, which can result in missing serious hypo/hyper-glycemic incidents [4].

In the past decade, researchers have investigated several new blood glucose level measurement techniques. These fall within one of two categories: minimally invasive and non-invasive [5]. Minimally invasive methods, such as the glucose-oxidase based electrochemical sensors, are painful and uncomfortable, suffer from delay artifacts and cause high socio-economic burdens [6].

As for the non-invasive techniques, some of these methods are not suitable for continuous monitoring as they require samples of saliva [7], urine [8], tears [9] and breath [10]. Other approaches such as, reverse iontophoresis [11], [12], bio-impedance spectroscopy [13], infrared spectroscopy [14], and ultrasound [15] were also investigated. So far, however, the existing solutions have failed to replace the glucometer as they lack the desired accuracy and stability, or they suffer from a large time lag [16], [17]. More recently, alternative solutions using electromagnetic based techniques are being developed as means to provide continuous and non-invasive monitoring of BGLs with enhanced accuracy [18]–[22]. Several microwave design approaches such as waveguides, dielectric probes and antennas [23]–[26] have been proposed in the literature. Other methods consist of employing planar filters and resonators. For these structures, extraction of the electrical properties of blood is achieved by placing the material under test (MUT) in close proximity to the resonators. Such placement changes the scattering parameters of the resonators in comparison to their free-space response. Hence, it leads to the extraction of the electrical properties of the loading MUT [27]. This measurement method provides a low-cost, compact-size and non-destructive tool for dielectric constant characterization, and it is suitable for non-contact measurements over the desired frequency range [27]. Other approaches such as waveguides, coaxial probes and electrodes may not be suitable for glucose sensing since they are either bulky, expensive or can disturb the MUTs [27]. In [28], [29] the proposed devices sense variations in glucose concentrations as shifts in the resonant frequency. The considered resonators exhibit promising results in terms of sensitivity and linear dependency towards glucose levels over a narrow range of frequencies.

In this paper, a flexible broadband reject filter design based on a modified log-periodic set of distributed complementary open loop resonators (OLRs) is proposed for sensing glucose levels across a broadband frequency range extending from 1.25 GHz to 2.65 GHz. A rigid band reject filter initially briefly presented in [30], characterizes dielectric material by relying on the filter's response at multiple frequencies. The wideband feature exhibited by the proposed flexible sensor increases the sensitivity and decreases the prediction error.

The novelty of the work presented in this paper is based on proposing a first of its kind miniaturized and flexible broadband RF-based sensor designed specifically for glucose monitoring. The broadband behavior enhances prediction accuracy by increasing the available set of critical features, which decreases the prediction error of blood glucose levels. Another advantage of the broadband response is its ability to provide a wide range of penetration depths ranging from 18 mm (higher frequencies) to 30 mm (lower frequencies). This is an important aspect that makes the filter more suitable and easily adaptable for varying users' physiological needs such as age and gender. Consequently, different set of frequencies may be selected for different users. To achieve the broadband response, four complementary modified OLRs are logarithmically scaled in relation to each other at the bottom layer of the structure [31], and a tapered feeding line is implemented on the top layer to further accentuate the sensor's broadband rejection response [32]. The OLRs are meandered [33] and perturbed [34] to exhibit an enhanced electric field distribution, which increases the sensitivity to glucose variations.

Statistical regression methods have been instrumental tools for electromagnetic applications [35]. We employed regression models that are developed using experimental data obtained from in-vitro and ex-vivo setups, and from healthy patients, subject to glucose tolerance tests. The proposed sensor displays a mean absolute relative difference between the reference and estimated glucose levels that is less than 4%. The predicted glucose levels also lie 100% within the clinically acceptable zones of the Clarke Error Grid. This is the first of a kind broadband reject flexible filter with enhanced electric field distribution for exceptional glucose level variations sensitivity.

## II. PROPOSED SENSOR

The proposed broadband reject filter, shown in Fig. 1, is a double-sided microstrip structure consisting of a feeding line (top layer), and a sensing area (bottom layer) that are separated by a dielectric layer. The filter is designed and simulated using Ansys Electronics Desktop [36]. The substrate is a flexible 0.25 mm-thick Rogers 3003 with a dielectric constant of 3 and a loss tangent equals to 0.001. The top layer comprises an exponentially tapered feed line that couples the magnetic flux density to the resonators underneath. The transmission line is adjusted based on tapering techniques [32] in order to enhance the broadband operation of the filter. The impedance  $Z_{L/2}$  and the line's characteristic impedance  $Z_0$  in (1) are associated with the widths  $W_{L/2}$ , and  $W_0$  as defined in Fig. 1. The position-dependent impedance  $Z(x)$  in (1) is obtained based on "a", which

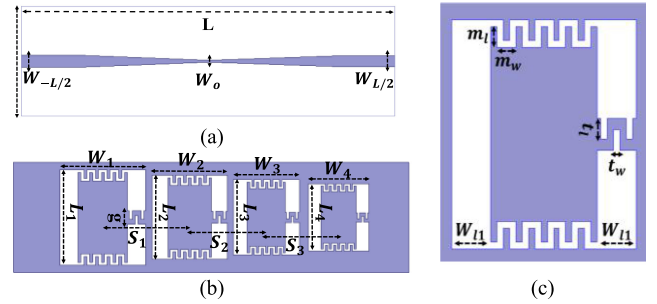


Fig. 1. (a) Feeding line. (b) Sensing area of the proposed filter. (c) Zoomed in schematic of largest OLR (right). Drawings are not to scale.

TABLE I  
PARAMETER VALUES OF THE PROPOSED SENSOR

Parameter	Value (mm)	Parameter	Value (mm)	Parameter	Value (mm)
$W$	30	$L_3$	17.6	$S_2$	13.8
$L$	65	$L_4$	15.5	$S_3$	12.15
$W_{L/2}$	0.63	$W_1$	16.15	$g$	1.3
$W_0$	0.35	$W_2$	14.2	$t_l$	0.8
$W_{l1}$	0.32	$W_3$	12.5	$t_w$	0.06
$L_1$	22.8	$W_4$	11	$m_l$	0.95
$L_2$	20	$S_1$	15.7	$m_w$	1.584

is the tapering coefficient defined in (2) [32].

$$Z(x) = Z_{L/2} \times e^{a|x|}, x \in \left[-\frac{L}{2}, \frac{L}{2}\right] \quad (1)$$

$$a = \frac{1}{L/2} \times \ln \left( \frac{Z_0}{Z_{L/2}} \right), Z_{L/2} = 50 \Omega \text{ and } Z_0 = 100 \Omega \quad (2)$$

The bottom layer, which constitutes the sensing side of the proposed filter, is a defected ground plane composed of four complementary OLRs. The dimensions and spacing of the incorporated OLRs follow a modified logarithmic periodic distribution as presented in (3);  $\tau$  is a scaling factor that affects the desired bandwidth  $B$  for the four OLRs [31]. The electrical length of the largest OLR is taken to be one-half the guided wavelength ( $\lambda_{\max}$ ) that corresponds to the lowest desired frequency of operation as shown in (4), where  $u_p$  is the phase velocity. We set  $\tau = 0.88$  and determine the dimensions of the proposed filter configuration according to (3) and (4) [31]. The dimensions of the proposed design are presented in Table I.

$$\frac{W_{n+1}}{W_n} = \frac{L_{n+1}}{L_n} = \frac{S_{n+1}}{S_n} = \frac{1}{\tau} \quad (3)$$

$$L_{\max} = \frac{\lambda_{\max}}{2} = \frac{u_p}{2f} \quad (4)$$

The human body is modeled as a lossy medium, characterized by the effective complex permittivity  $\epsilon_{eff} = \epsilon_0 \epsilon_r (1 - j \tan \delta)$  where the real part signifies the stored electric field energy and the imaginary part accounts for medium losses. For the proposed sensor to be sensitive to BGL variations, it must be sensitive to  $\epsilon_{eff}$ . The placement of the sensor near the MUT perturbs its field strength and distribution versus frequency. The higher the

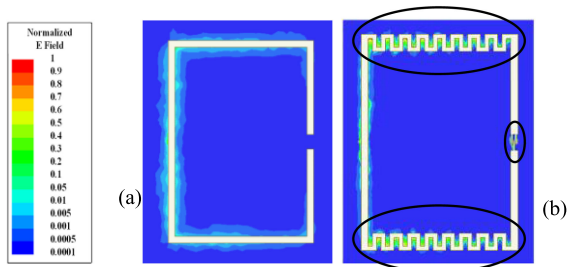


Fig. 2. Normalized electric field intensity distributed over the bottom layer of (a) regular and (b) modified complementary OLR.

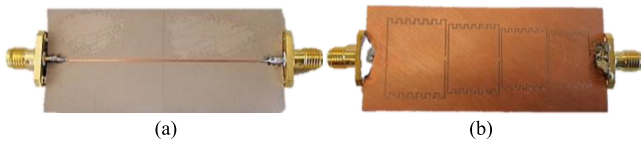


Fig. 3. (a) Top layer and (b) bottom layer of the fabricated prototype of the proposed design on Rogers 3003 substrate.

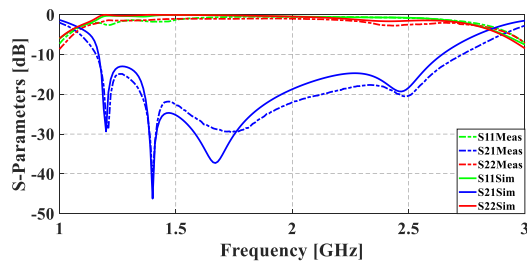


Fig. 4. Free space magnitude response of the proposed sensor.

E field intensity, the greater is the sensitivity [37]. To upsurge the distribution of the fields, the resonators are etched from the ground plane. This complementary configuration spreads the induced fields across the bottom side, and hence provides a higher interaction area with the loading MUT. Moreover, by perturbing the resonators and meandering two sides of the resonators as shown in Fig. 2, the magnitudes of the induced fields tend to increase, thus leading to enhanced sensitivity levels [30]. Furthermore, the implementation of these series L-C meandered lines produces a 35% reduction in the size of the OLRs.

### III. EXPERIMENTAL SETUPS

To validate the performance of the proposed filter, a  $3 \times 6.5 \text{ cm}^2$  prototype is fabricated as illustrated in Fig. 3 based on the dimensions provided in Table I. The prototype is first measured in free space using the Keysight Fieldfox N9914A RF analyzer [38], where a good agreement between the simulated and measured S-parameters is obtained as shown in Fig. 4. A clear broadband reject response is demonstrated in the 1.25–2.65 GHz frequency range. Furthermore, the operation of the flexible filter is validated by monitoring its response under different bending setups. The proposed sensor presents consistent performance for different bent states. This is verified in Fig. 5, where we note low variation ( $\sim 0.2 \text{ dB}$ ) in the measured S-parameter response upon

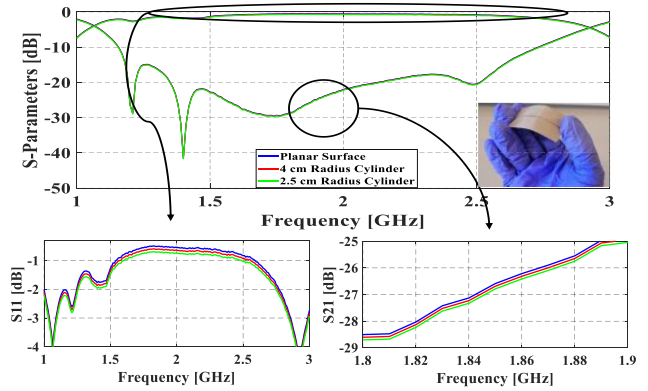


Fig. 5. Measured reflection and transmission magnitude for different cylinders' radii. Direction of bending is as shown in the figure.

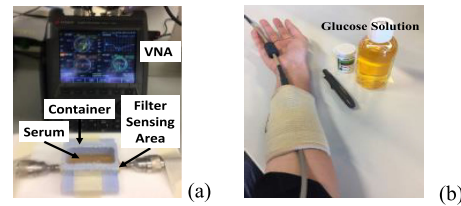


Fig. 6. (a) Experimental setup of serum measurements. (b) Setup of the in-vivo measurements: proposed sensor placed on the lower arm of the patient and connected via two cables to the VNA.

bending. This proves the sensor's suitability for operation under bent conditions, thereby enabling its utilization as a wearable sensing apparel.

To validate the ability of the proposed sensor in carrying out continuous and non-invasive glucose monitoring measurements, the realized prototype is tested in-vitro, ex-vivo and in-vivo setups. For each illustrated setup, the changes in the sensor's measured S-parameters are tracked and mapped to glucose level variations using machine learning algorithms as discussed in Section IV.

#### A. In-Vitro Experiments: Serum Measurements

The first measurement setup is initiated by relying on serum as a MUT; serum is a known liquid that mimics the critical composition of the blood [39]. A serum-filled foam container is positioned on top of the bottom layer of the sensor as shown in Fig. 6(a). Small increments of glucose powder, which result in a 10 mg/dL glucose variation, are added to the serum on a ten-minutes-interval basis and the sensor's S-parameters are conveniently measured within each interval. As a first test, baseline measurements are executed. This is conducted by measuring the sensors' S-parameters in the absence of the foam container, then by placing an empty container on the bottom layer of the sensor (sensing area), and finally by filling the container with serum. This test is performed to ensure that the sensor under study maintains its free space responses, with and without the empty foam container. A shift in frequency occurs only when the serum is added. This behavior is noted for both the magnitude and phase of the sensor's S-parameters. Following

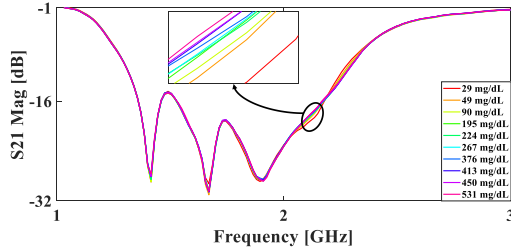


Fig. 7.  $S_{21}$  magnitude response for different BG concentrations.

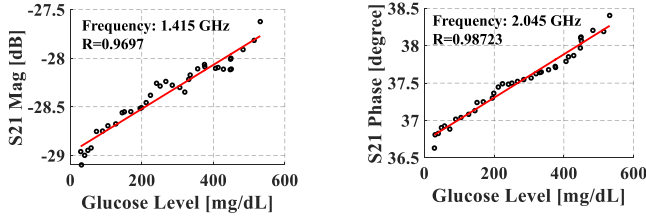


Fig. 8. Correlation between the sensor's response and glucose concentrations at different frequencies for in-vitro measurements data.

that, the filter's response is recorded for 37 observation points corresponding to different glucose levels ranging from 29 mg/dl to 531 mg/dL covering the whole hypo- to hyperglycemic range. Fig. 7 displays the transmission coefficient response of the proposed sensor for different glucose concentrations. We also note a strong correlation between the glucose levels measured using the glucometer and the filter's response. The strength of the correlation is quantified using Pearson's linear correlation coefficient (PCC)  $R = \frac{C_{xy}}{\sigma_x \sigma_y}$  [40], where  $C_{xy}$  represents the covariance between the filter's S-parameters (X) and the reference GLs (Y), and  $\sigma_x$  and  $\sigma_y$  denote the standard deviations of X and Y, respectively. Similarly to [41]–[43], high correlation values are recorded. However, this correlation is not restricted to one narrow band, but rather observed over a wide range of frequencies as seen in Fig. 8 for 37 different glucose levels.

### B. Movement, Position, Temperature and Chemical Interference Tests:

In this section we study the effects of environmental (temperature), systematic (position and movement) and chemical (potential interference) variables on the filters' response and sensitivity to glucose detection.

1) *Effect of Position and Movement Experiment:* The proposed filter is intended to be fixed inside an armband, which will enhance the sensor's adaptability to body movements. Additionally, during experiments, the filter is separated from the skin surface by a flexible foam allowing the filter to move with the human body. To test the sensor's response to movement, two different sets of measurements are performed. In the first measurement setup of Fig. 9(a), the filter is fixed on the arm inside an armband and is tested over arm movement with two different angles. The filter maintained a stable performance for the two arm configurations, as shown in Fig. 9(a), with minimal

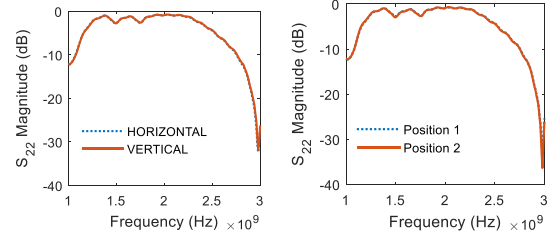


Fig. 9. The effect of (a) moving the arm and (b) changing the position of the flexible filter on the S-parameters response.

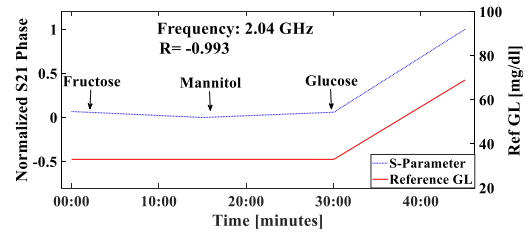


Fig. 10. Correlation between the sensor's response and different types of sugar.

difference between the filter's S-parameters response. Measurements with the filter positioned at two different locations on the arm are also presented in Fig. 9(b) showing that the change of the filter position did not affect the S-parameters.

2) *Chemical Interference Tests:* A selectivity experiment is also performed during which 50 mg/dl of fructose, mannitol and glucose is successively added to the serum solution. In this experiment, the filter is positioned exactly as described for the in-vitro setup. The results prove more selectivity toward glucose than other types of sugar including fructose and mannitol as shown in Fig. 10.

3) *Temperature Effect Experiment:* To study the effect of the ambient temperature, the filter's response is also monitored at different temperature levels when loaded with a serum solution. The temperature is changed from 19.8 to 23.7°C in a controlled temperature room. A minimal effect of the temperature change on the filter's S-parameters is noted as shown in Fig. 11. Such effect can be easily calibrated as discussed in [44].

### C. Ex-Vivo Experiments: Animal Tissues

All animal procedures are conducted in accordance with the United States Public Health Service's Policy on Humane Care and Use of Laboratory Animals and were approved by the Institutional Animal Care and Use Committee at the American University of Beirut. In this experiment, skin, fat and muscle tissues are extracted from two healthy euthanized rats. Hair is removed using depilatory cream before measurements. The area of the sample is about 1.8 cm  $\times$  6 cm. The extracted

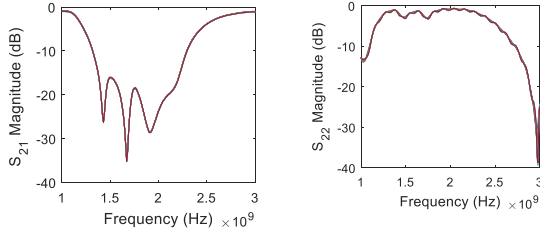


Fig. 11. The effect of changing the room temperature on the flexible filter's S-parameters.

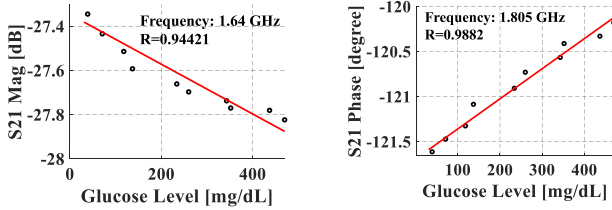


Fig. 12. Correlation between the response of the sensor and the glucose concentrations based on the data collected from ex-vivo measurements.

tissues are fixed in a foam container, placed on top of the sensor and beneath a 4 mm layer of serum. Glucose is added to the serum layer resulting in 45 mg/dl incremental steps in the glucose level, and the S-parameters are measured. During this experiment, we recorded a total of 12 observation points to shorten the experiment time and avoid tissue deterioration. The linear correlation between the response of the sensor and the glucose level is maintained as illustrated in Fig. 12 for a variety of frequencies over the operating range.

#### D. In-Vivo Experiments: Clinical Measurements Design

For in-vivo testing, six healthy volunteers are recruited to participate in a limited and controlled clinical trial. Subjects are considered eligible if their age ranges between 18 and 70 years, are able to provide informed consent, have HbA1c levels lower than 6.2%, and show no sign of dyslipidemia. There are no restrictions on either race, sex or ethnicity. Substance abuse, lactation, pregnancy, and being part of an interventional trial are the exclusive criteria.

Approval from the Institutional Review Board [45] at the American University of Beirut is sought before initiation of these trials. Volunteers arrive to the clinical study unit in the morning after fasting for at least 8 hours. Measurement of blood glucose levels is initially performed using the standard techniques by relying on an Accu-Check glucometer [46]. Afterwards, the sensor under test is attached to the lower arm of the volunteer as illustrated in Fig. 6(b). Subsequently, glucose is orally ingested as a concentrated glucose drink that contains 75 g of glucose dissolved in 200 mL of water. This induces a hyperglycemic excursion to a BGL target of 185–220 mg/dL. These levels are expected to drop to reasonably lower values within 2 hours. Readings from the sensor are collected every 5 minutes, and reference BGLs are measured at intervals of 15 minutes using the glucometer [47]. Typically, few reference invasive glucose level

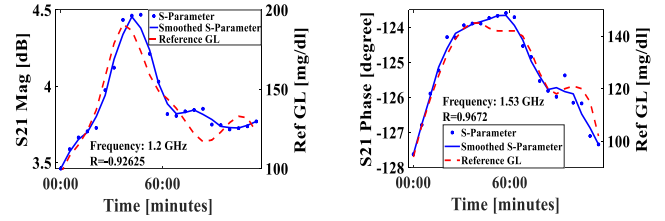


Fig. 13. Correlation between the response of the sensor and the glucose concentrations based on the data collected from in-vivo measurements. The smoothing is done solely for observation purposes.

points are collected per patient during a given OGTT per general recommendation, as was the case in other works [48]–[50]. A total of 23 observations per OGTT are recorded using our device, one every five minutes. Out of these, 9 reference value points are directly obtained using the glucometer. The remaining 14 reference glucose points are interpolated using cubic splines [51]. During the process, patients are asked to stay tranquil and with minimal physical movements. The room temperature is set to  $23 \pm 0.5^\circ\text{C}$ . This oral glucose tolerance test (OGTT), spans a period of 2 hours, and is performed twice for each subject on two separate days.

The proposed sensor's response demonstrates a clear correlation with the reference BGLs. High PCC values are reported at multiple frequencies for the same OGTTs. This is demonstrated in Fig. 13 for the different patients. The red lines are the invasively measured BGLs, and the dots are the S-parameter values at a specific frequency. The blue line corresponds to the smoothed S-parameters. This good correlation is achieved with an average sensitivity of 0.01 dB/mg/dL and  $0.09^\circ/\text{mg/dL}$  over different frequencies.

#### IV. FROM S-PARAMETERS TO GLUCOSE LEVELS: STATISTICAL REGRESSION MODEL

For glucose estimation, we tested different regression techniques to establish a dependence between the filter's S-parameters (input variables,  $X, \in \mathbb{R}$ ) and reference glucose levels (GL) (output variable,  $y \in \mathbb{R}$ ). Data processing and regression modeling are carried out using MATLAB R2017a [52].

##### A. Data collection and Processing

Data collection and data processing were implemented following the pseudocode below, where  $X$  represents the normalized feature vectors and  $Y$  denotes the reference glucose level dependent variable.

For each OGTT for a given patient,

##### Data collection Phase (Preprocessing):

- Every 5 minutes collect from the sensor the  $i^{\text{th}}$  observation data points:

$\mathbf{X}_{S:pre}(i, :) = \{\mathbf{x}_{S:pre}^j(i, :)\}$  with a total of 1206 features in  $\mathbf{X}_{S:pre}$ , where  $i \neq [1, 23]$  represents the observation number,  $j \neq [1, 6]$  represents each of  $S_{11}$ ,  $S_{21}$ ,  $S_{22}$ , magnitudes and phase respectively, and  $\mathbf{x}_{S:pre}^j$  comprises 201 features obtained over the frequency range [1–3] GHz,

- Every 15 minutes, perform a standard measurement, to collect the reference GL, collect:  $y_{ref:meas}(m)$

#### Data Processing Phase:

- $Y = \{y_{ref}(i)\}$ , where  $y_{ref}(i)$  represents the reference glucose level obtained from  $y_{ref:meas}(m)$  and/or using cubic splines [51] for the  $i^{\text{th}}$  observation point if  $y_{ref:meas}(m)$  is missing at that time point to obtain a total of 23 ref GL over the duration of the OGTT.
- $X_s = \{X_s^k\}$  is the set of 126 feature vectors obtained by sampling  $x_{S:pre}^j$  at steps of 0.1 GHz for all  $j$ . Therefore,  $X_s^k(i)$  is the value of feature  $k$  for observation  $i$ , where  $k \neq [1, 126]$ , and  $i \neq [1, 23]$ .
- We normalize each feature vector,  $X_s^k$ , across all observations as follows:

$$X_{norm}^k(i) = \frac{X_s^k(i) - \min(X_s^k)}{\max(X_s^k) - \min(X_s^k)}$$

- $X = \{X_{norm}^k\}$

#### B. Regression Modeling

To choose the most adequate regression technique, two important aspects of the collected data must be taken into consideration. 1) The small size of the dataset due to the limited number of reference glucose points, where we collected 23 points in each OGTT to limit the discomfort caused by the patients' fingers pricking; and 2) the high dimensionality of the dataset where we have 1206 features for each observation point. Based on previous literature [53]–[55], several regression techniques including Locally Weighted Partial Least Squares (LW-PLS) [53], Least Absolute Shrinkage, Selection Operator (LASSO) [54] and Gaussian Processes (GP) [55], [56], are evaluated. PLS is a regression methodology that deals with dimensionality reduction problem. It creates new components that explain the variability in the input variables while taking the relation between the output and input variables into consideration. In our application, minimizing the error of the low glucose levels estimation is our top priority, hence we are interested in minimizing the relative error, rather than the absolute error. For this reason, we considered the locally weighted PLS (LW-PLS), where PLS is utilized for local modeling relying mainly on the similarity between the new query and the existing data points. Whenever an estimation is needed for a new query, a local model is created from samples located around the query. The definition of the similarity between the query and the existing samples is based on the weighted Euclidean distance.

LASSO is another linear regression method that performs  $L_1$  regularization and feature selection implicitly. This methodology applies sparsity and therefore sets many input variables coefficients to zero leaving only the ones, which have strong effect on the estimation of GLs. Since the number of features (126) is still large compared with the number of data points, feature selection is important to avoid overfitting. LASSO algorithm and LW-PLS implicitly perform critical feature/component ordering. We rely on a 10-fold cross-validation to find the best number of critical features [57].

Gaussian process regression (GPR) is a probabilistic nonlinear kernel-based regression approach that has shown its ability to

provide high performance when applied on a small dataset [55], [56]. GPR assumes that the model function  $f(x)$  is distributed as a Gaussian process thereby reflecting uncertainty towards the function. The dataset variables are related one to the other using a covariance function  $k(x, x_q)$ , also known as the kernel function. It offers a similarity measure between the points. The kernel function is usually defined by a set of hyperparameters  $\theta$  including the length-scale and signal variance. When a new query requires estimation, the distant dataset points will have a negligible effect on the estimation of the new query output. We evaluate five different kernel functions: Exponential, squared exponential, matern 32, matern 52 and rational quadratic [52].

Since GPR doesn't perform implicitly feature selection, we perform feature selection explicitly and the model with the set of features and the kernel that minimizes a 10 fold cross validation score is selected. Two feature selection techniques were tested. The filter method [58] consists of sorting the features based on their maximum correlation or relevance with respect to the outcome and then performs CV to find the smallest best set of features in the specified order. A more exhaustive yet robust technique is the wrapper method [58]. The best set of critical features is selected solely based on the regression model outcome. At each step, the wrapper method identifies the next best feature for a given kernel function.

For this analysis, each dataset is divided into two subsets: training (2/3) and testing (1/3). The first data subset is used to identify the model's parameters and the second is used to test the models over "unseen" data. This process is repeated 10 times in order to cover most observations [59]. The output of the model are the individual estimated glucose level points along with their mean values from the different replications.

#### C. Performance Metrics

The model accuracy is validated using the mean absolute relative difference (MARD) in (5), commonly used in the diabetes community;  $n$  is the number of sample points.

$$MARD = 100 * \frac{1}{n} \sum_{i=1}^n \frac{|BGL_{Glucometer} - BGL_{Estimated}|}{|BGL_{Glucometer}|} \quad (5)$$

To evaluate the clinical accuracy of the proposed filter design estimates, Clarke Error Grid analysis is considered [60]. The technique evaluates the clinical accuracy of the proposed design measurements against those of the noninvasive blood glucose meter. In this work, the reference measurements are considered to be those obtained using the commercial glucometer. For the Clarke Error Grid, reference values are displayed on the x-axis and predicted values are presented on the y-axis. Points lying on the diagonal signify a perfect match between reference and predicted values. The grid is divided into five zones. Zones A and B are clinically acceptable. Zones C, D and E are potentially dangerous.

#### D. Results

Data collected from in-vitro measurements on serum is used to compare the different regression techniques. We note that the GPR-based model outperforms the other methods as seen

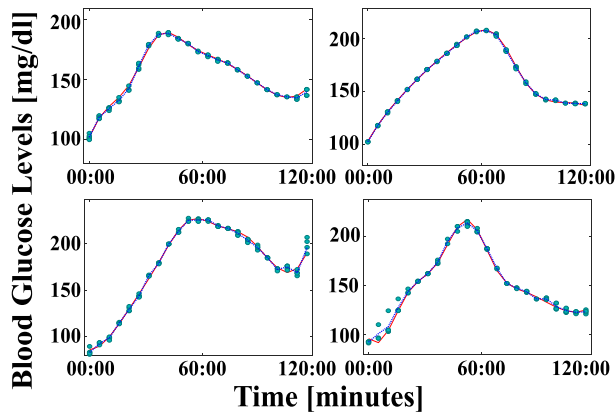


Fig. 14. Blood glucose levels profiles for four different OGTTs. Each plot includes the reference (red line), estimated (dots), and average estimated (blue line) glucose levels.

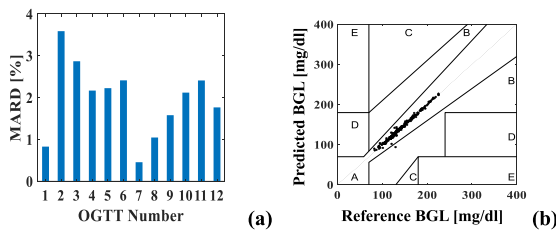


Fig. 15. (a) Individual MARD for all twelve OGTTs. (b) Clarke error grid obtained for data predicted using GPR.

by the MARD values (*i.e.* LW-PLS: 11.26%; LASSO: 8.31%; GPR: 5.12%). In what follows, we present the results of the GPR model applied to the in-vivo measurements. The number of selected features was on average found to be 12 features for the OGTT experiments; 76% of the selected features were based on S21 magnitude and phase parameters, and the other 24% were selected from the remaining S parameters. Fig. 14 presents the individual BGL profiles as function of time for both the estimated as well as the reference BGLs. For each profile, we note a rapid increase in glucose values from the fasting level to a peak value, and then followed by a decrease in the glucose levels. The solid lines represent the invasively measured BGLs, and the dashed lines are the estimated values using GP. The dots correspond to the predicted values using the aforementioned 10 randomly generated test and training data sets for a given OGTT. It is apparent that the estimated glucose concentration, matches well the reference glucose levels.

The MARD values for all the OGTTs are plotted in Fig. 15(a). The recorded MARD values range between 0.45% and 3.65%, and have an overall mean value of 1.97% for all the 12 OGTTs. The generated Clarke grid obtained using the data collected from the clinical trials is shown in Fig. 15(b). It is noted that 275 of 276 predicted data points (99.43%) lie in zone A, and one point lies in zone B. This signifies that all the points are in the clinically acceptable regions. A leave-one-out cross-validation analysis also demonstrates a MARD of 1.09% and 100% data

points in zone A. These results show exceptional accuracy of the proposed microwave sensor and accompanying model.

## V. CONCLUSION

This paper presents a novel flexible broadband reject filter that operates between 1.25 and 2.65 GHz. The flexibility and free-space response of the filter is confirmed by testing its prototype's response for different bending angles, where measured results agree well with simulated data. The behavior of the proposed broadband reject filter as glucose sensing sensor is tested using in-vitro, ex-vivo and in-vivo experiments. Excellent correlation between the proposed sensor's S-parameters and glucose level variations is achieved. Gaussian process regression models are developed using experimental data, and the predicted glucose levels are found to be 100% in the clinically acceptable regions of the Clarke Error Grid. This is to our knowledge the first of a kind broadband reject flexible filter that exhibits exceptional accuracy in tracking the variations of glucose level in the blood as validated pre-clinically and clinically.

## REFERENCES

- [1] "About Diabetes," Int. Diabetes Federation., published 2019, last updated Feb. 2020. Accessed: Sep. 17, 2020. [Online]. Available: <https://www.idf.org/aboutdiabetes/what-is-diabetes/facts-figures.html>
- [2] "Diabetes the Basics," Diabetes U.K., 2019, Accessed: 3 Jan. 2020. [Online]. Available: <http://www.diabetes.org.uk/Diabetes-the-basics/>
- [3] M. J. Fowler, "Microvascular and macrovascular complications of diabetes," *Clin. Diabetes*, vol. 29, no. 3, pp. 116–122, Jul. 2011.
- [4] R. A. Gabbay, "New developments in home glucose monitoring: minimizing the pain," *Can. J. Diabetes*, vol. 27, no. 3, pp. 271–276, 2003.
- [5] A. Nawaz, P. Øhlckers, S. Sælid, M. Jacobsen, and M. N. Akram, "Review: Non-invasive continuous blood glucose measurement techniques," *J. Bioinf. Diabetes*, vol. 1, no. 3, pp. 1–27, Jul. 2016.
- [6] G. Cappon, M. Vettoretti, G. Sparacino, and A. Facchinetti, "Continuous glucose monitoring sensors for diabetes management: A review of technologies and applications," *Diabetes Metabolism J.*, vol. 43, no. 4, pp. 383–397, Aug. 2019.
- [7] D. Bruen, C. Delaney, L. Florea, and D. Diamond, "Glucose sensing for diabetes monitoring: Recent developments," *Sensors*, vol. 17, no. 8, Aug. 2017, Art. no. 1866.
- [8] J. P. Comer, "Semi-quantitative specific test paper for glucose in urine," *Analytical Chemistry*, vol. 28, no. 11, pp. 1748–1750, Nov. 1956.
- [9] H. Yao, A. J. Shum, M. Cowan, I. Lähdesmäki, and B. A. Parviz, "A contact lens with embedded sensor for monitoring tear glucose level," *Biosensors Bioelectronics*, vol. 26, no. 7, pp. 3290–3296, Mar. 2011.
- [10] C. Todd, P. Salvetti, K. Naylor, and M. Albatat, "Towards non-invasive extraction and determination of blood glucose levels," *Bioengineering*, vol. 4, no. 4, pp. 82–92, Sep. 2017.
- [11] A. Siegel, R. H. Guy, and M. B. Delgado-Charro, "Noninvasive glucose monitoring by reverse iontophoresis in vivo: Application of the internal standard concept," *Clin. Chemistry*, vol. 50, no. 8, pp. 1383–1390, Aug. 2004.
- [12] L. Lipani *et al.*, "Non-invasive, transdermal, path-selective and specific glucose monitoring via a graphene-based platform," *Nature Nanotechnol.*, vol. 13, no. 6, pp. 504–511, Apr. 2018.
- [13] A. Caduff *et al.*, "Non-invasive glucose monitoring in patients with Type 1 diabetes: A Multisensor system combining sensors for dielectric and optical characterisation of skin," *Biosensors Bioelectronics*, vol. 24, no. 9, pp. 2778–2784, May 2009.
- [14] R. Kasahara, S. Kino, S. Soyama, and Y. Matsuura, "Noninvasive glucose monitoring using mid-infrared absorption spectroscopy based on a few wavenumbers," *Biomed. Opt. Express*, vol. 9, no. 1, pp. 289–302, Jan. 2018.
- [15] J. Kost, M. Pishko, R. A. Gabbay, R. Langer, and S. Mitragotri, "Transdermal monitoring of glucose and other analytes using ultrasound," *Nature Med.*, vol. 6, no. 3, pp. 347–350, Mar. 2000.





**Jessica Hanna** received the B.Sc. and M.Eng. degrees in biomedical instrumentation from the Holy Spirit University of Kaslik, Jounieh, Lebanon, in 2013 and 2015, respectively. She is currently working toward the Ph.D. degree with the Biomedical Engineering Program, American University of Beirut, Beirut, Lebanon. Her main research interests include design and fabrication of RF-based sensors for non-invasive, continuous glucose monitoring, signal processing and data analysis.



**Joseph Costantine** (Senior Member, IEEE) received the bachelor's degree from Lebanese University, Beirut, Lebanon, the master's degree from American University of Beirut, Beirut, Lebanon, and the Ph.D. degree from The University of New Mexico, Albuquerque, NM, USA, in 2009. He is currently an Associate Professor with the Department of Electrical and Computer Engineering, American University of Beirut. He has seven Provisional and Full U.S. patents. He has authored or coauthored two books, one book chapter, and more than 150 journal and

conference papers. His research interests reside in reconfigurable antennas, cognitive radio, RF energy harvesting systems, antennas and rectennas for IoT devices, RF systems for biomedical devices, wireless characterization of dielectric material and deployable antennas for small satellites. He has been an Associate Editor for the IEEE ANTENNAS AND WIRELESS PROPAGATION LETTERS since July 2018. He received many awards and honors throughout his career including the 2008 IEEE Albuquerque chapter Outstanding Graduate Award, the three year (2011–2013) Air Force summer faculty fellowship with Kirtland's Space Vehicles Directorate in NM, USA, the 2017 First Prize at the Idea-thon of International Healthcare Industry Forum, the 2019 Excellence in Teaching Award from American University of Beirut, and the 2018 and 2020 STC Science and Technology Innovation awards. In addition, he has been selected by the World Economic Forum as one of the world's leading young scientists for the year 2020.



**Rouwaida Kanj** (Senior Member, IEEE) received the M.S. and Ph.D. degrees in electrical engineering from the University of Illinois at Urbana-Champaign, Champaign, IL, USA, in 2000 and 2004, respectively. She is currently an Associate Professor with the American University of Beirut, Beirut, Lebanon. From 2004 to 2012, she was a Research Staff Member with IBM Austin Research Labs. Her research work focuses on advanced algorithmic research and development and smart analytics methodologies for design for manufacturability reliability and yield with

emphasis on statistical analysis, optimization and rare fail event estimation for microprocessor memory designs along with machine learning applications for very large scale integration. This is in addition to her earlier work on noise modeling and characterization of CMOS designs. She was the recipient of three IBM Ph.D. Fellowships, is the author of more than 70 technical papers, 30 issued US patents, and several pending patents. She received an Outstanding Technical Achievement Award and six Invention Plateau awards from IBM. She received the prestigious IEEE/ACM William J. McCalla ICCAD Best Paper Award in 2009, and two IEEE ISQED Best Paper awards in 2006 and 2014.



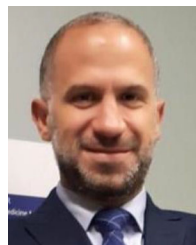
**Youssef Tawk** received the B.Eng. degree (with highest distinction) from Notre Dame University Louaize, Zouk Mosbeh, Lebanon, in 2006, the M.Eng. degree from the American University of Beirut, Beirut, Lebanon, in 2007, and the Ph.D. degree from the University of New Mexico, Albuquerque, NM, USA, in 2011. He is currently an Assistant Professor with the ECE Department, American University of Beirut. His research interests include reconfigurable RF systems for microwave and mm-wave applications, cognitive radio, optically controlled RF components, phased

arrays, and phase shifters based on smart RF materials. He is an Associate Editor of the Wiley *Microwave and Optical Technology Letters*. He is the co-author of two books and one book chapter, and co-inventor on seven US patents. Throughout his education and career, he has received many awards and honors such as the 2018 and 2014 Science and Technology Innovation award for his patents on reconfigurable microwave filters and optically controlled antenna systems in addition to the 2011 IEEE Albuquerque Chapter Outstanding Graduate award. He has more than 140 IEEE journals and conference papers many of which received finalist positions and honorable mentions in several paper contests.



**Ali H. Ramadan** received the Ph.D. degree in electrical and computer engineering from the American University of Beirut, Beirut, Lebanon, in 2014. In 2010, he joined the Cognitive Radio Research Group, Department of Electrical and Computer Engineering, The University of New Mexico, Albuquerque, NM, USA, where he was a Ph.D. Exchange Research Scholar from 2010 to 2013. In 2014, he joined the Department of Electrical and Computer Engineering, American University of Beirut, as a Postdoctoral Fellow, where he held a Research Associate position, in

2017. He is currently an Assistant Professor with the Department of Electrical Engineering, Fahad Bin Sultan University, Tabuk, Saudi Arabia. His current research interests include wireless power transfer (WPT), bio-electromagnetics, reconfigurable RF front-end transceivers for Internet of Things (IoT) applications, and phased antenna arrays.



**Assaad A. Eid** received the doctorate degree in metabolism and endocrinology from the Faculty of Medicine, Claude Bernard University, Lyon, France, in 2006. After that he joined the Department of Medicine/Nephrology, University of Texas Health Science Center at San Antonio for his fellowship. He is currently involved in cutting-edge basic, translational and clinical science research in the field of diabetes and diabetic complications. In October 2010, he was appointed as an Assistant Professor with the Faculty of Medicine, American University of Beirut

(AUB-FM), and then was promoted to the rank of Associate Professor in 2015. Furthermore, he is currently the founding Co-Director of the AUB diabetes and the Director of the Faculty of Medicine Master programs. His work is funded by several national and international research grants and his name appears on more than 60 publications and book chapters as well as three patents. In recognition to his contribution to research and training, he was elected as a member in the Inter-Academy Medical Panel - Young Physician Leaders and as a Young Affiliate Member of The World Academy of Sciences for the developing world (TWAS). Besides, in 2017, he was appointed as a Visiting Professor with Paris Descartes University, Paris, France and in 2018 he joined the Neuronetwork for Emerging Medicine, University of Michigan at Ann Arbor as International Associate.